SECTION 1

BIOMASS

ALLOMETRY BETWEEN CROWN AREA AND STEM DIAMETER AND ABOVE-GROUND BIOMASS ESTIMATION IN MANGROVE FORESTS DERIVED FROM HIGH-RESOLUTION SATELLITE DATA

Yasumasa HIRATA[a], Ryuichi TABUCHI[b], Pipat PATANAPONPAIBOON[c], Sasitorn POUNGPARN[c], Reiji YONEDA[d], Yoshimi FUJIOKA[e]

[a]Forestry and Forest Products Research Institute, Bureau of Climate Change, 1 Matsunosato, Tsukuba, 305-8687 Japan, phone: +81-29-829-8330, fax: +81-29-874-3720, e-mail: hirat09@affrc.go.jp
[b]Japan International Research Center for Agricultural Science, Forestry Division, 1-1 Ohwashi, Tsukuba, 305-8686, Japan, phone: +81-29-838-6309, e-mail: tabuchi@ffpri.affrc.go.jp
[c]Chulalongkorn University, Faculty of Science, Bangkok, 10330, Thailand, phone: +66-2-218-5478, fax: +66-2-253-1874, e-mail: Pipat.P@chula.ac.th, sasi_p_p@hotmail.com
[d] Forestry and Forest Products Research Institute, Bureau of International Partnership, 1 Matsunosato, Tsukuba, 305-8687 Japan, phone: +81-29-829-8328, fax: +81-29-873-3797, e-mail: joneda@affrc.go.jp
[e]National Research Institute of Aquaculture, Minami-ise, Mie 516-0193, Japan, phone: +81-599-66-1830, fax: +81-599-66-1962, e-mail: fujioka@affrc.go.jp

ABSTRACT

Mangrove forests in tropical and subtropical countries play important roles from the viewpoint of ecosystem services such as water quality maintenance, storm wave protection, fish habitat and ecotourism activities as well as carbon stocking. Several mapping techniques of mangrove area using satellite sensor with a couple of 10-meters ground resolution, i.e. Landsat and SPOT, were developed to protect, restore and monitor costal ecosystem in previous studies (Green et al., 1998; Gao 1999; Saito et al., 2003). The new generation of high resolution satellite data of finer ground resolution than 1-m × 1-m such as IKONOS and QuickBird opened a new era for taking forest inventory and assessing forest biodiversity with remote sensing at landscape level. Forest inventory of mangrove forests is sometimes attended by the difficulty of the access because of the site environment and the complexity of the root system. Therefore, it is expected that high resolution satellite data are applied to the understanding of the present condition of mangrove forests as well as their dynamics (Rodriguez and Feller, 2004) and the classification of tree species using their properties of reflectance (Wang et al., 2004a; Dahdouh-Guebas et al., 2005). Wang et al., (2004b) indicated that both IKONOS and QuickBird data were suitable for classification of mangrove species from comparison of the results of texture analysis, likelihood classification and object-oriented classification.

To estimate tree biomass, we need some allometric relationships. Normally, we estimate it from the stem diameter and tree height. But we can only observe directly crown diameter and tree number from high-resolution satellite data. Therefore, we should estimate stem diameter and tree height using allometric relationships between crown area and stem diameter or between stem diameter and tree height.In this study, we present methods to identify crown area of mangrove from high-resolution satellite data

and to estimate above-ground biomass of mangrove forest with allometric equation between derived crown area and stem diameter.

The study area is located in the coastal zone of Ranong, Thailand. Twenty-three 0.04-ha sample plots were established and stem diameter of all trees and tree height of a part of them were measured in the field. The mean stem diameters of sample plots range from 9.5 to 31.1 cm and the densities from 106 to 3700 trees/ha. Dominant species of mangrove are *Rhizophora apiculata* Bl., *Rhizophora mucronata* Lamk., *Bruguiera cylindrica* (L.) Blume, *Bruguiera parvifola* (Roxb.) Wight et Arnold ex Griffith and *Xylocarpus granatum* Koenig.

QuickBird panchromatic data were acquired on 15 October 2006. A reversal image of QuickBird panchromatic data, calculated by subtracting each DN of the original data from the maximum value of DN in the data for each pixel (Wang et al., 2004c), was prepared to apply a watershed method for extraction of the individual crown areas. The mask of non-tree areas was used to avoid overestimating the crown area. Polygons of crowns and a polygon of a sample plot were superimposed and polygons of the inside of crown or partial inside of the plot were extracted in each sample plot. Finally, data sets of crown polygons were prepared for the sample plots. In general, the biomass of a tree is estimated from the stem diameter and tree height, while tree height is commonly determined from a height-diameter curve. Therefore, we need to estimate the stem diameter from individual crowns. An allometric model for relating measurable variables is commonly used for forest inventories and ecological studies (Ketterings et al., 2001). This model can be expressed as follows:

$$E(y) = ax^b \tag{1}$$

where x is the independent variable, y is the dependent variable and a and b are estimated parameters. Here, we investigated the allometric relationship between crown area obtained from QuickBird panchromatic data and the stem diameter measured in field survey for 23 sample plots. We assumed that extracted crown areas corresponded to measured stem diameters according to their sizes from the largest tree and suppressed trees could not be observed, i.e., their crowns had no area in the image. Using a data set of the stem diameters and crown areas estimated from QuickBird panchromatic data, parameters "*a*" and "*b*" in Equation (1) for each sample plot were estimated with the least-squares method respectively.

Komiyama et al. (1988) investigated the weight of each organ for mangrove species from some sampling trees and introduced formulas as bellows;

wS, wB,wPR and wF = a(D2H)b (2)
wL = 1/(a/ D2H+b) (3)

where,

wS :weight of stem
wB :weight of branches
wL :weight of leaves

wPR :weight of prop roots
wF :weight of fruits

and *a* and *b* are estimated parameters.

The weight of each organ by species was estimated from Eq. (2) or (3) using two variables, i.e. stem diameter and tree height with the estimated parameters, while tree height was introduced from diameter-height curve which was obtained from field survey. We calculated aboveground biomass (B_a) of a tree as the sum of these weights.

$$Ba=wS+wB+wL+wPR+wF \tag{4}$$

Above-ground biomass of sample plots obtained from stem diameter and tree height, which were estimated from QuickBird panchromatic data, was plotted against the biomass derived from the field measurements. The regression line that was fitted to the data by the least-squares method had an intercept of 63 ton/ha and a slope of 0.69 (R^2=0.66).

The accuracy of the biomass estimation seems to depend on the amount of the suppressed trees. Indeed, the number of trees in the study plots, which was extracted from the QuickBird data respectively, was smaller than the actual number of trees. Particularly, if trees of second layer are hidden by canopy layer, uncounted biomass occupies quit large part of estimation. Here, we used the watershed method to identify crown area. This is one of most common methods for this purpose, however, we should recognize that crown conditions are obviously different by individual trees. Some large trees are regards as multiple trees because of some divided crowns. When canopy surface is comparatively flat, canopy is not divided suitably for the limitation of the method. Nevertheless these problems, the results indicated the possibility of utilization of high-resolution satellite data to estimate the above-ground biomass of mangrove forest.

Keywords: allometry, above-ground biomass, crown area, high-resolution satellite data, mangrove, stem diameter

REFERENCES

Dahdouh-Guebas, F., Hiel, E.V., Chen, J.C.-W., Jayatissa, L.P. and Koedam, N. 2005. Qualitative distinction of congeneric and introgressive mangrove species in mixed patchy forest assemblages using high spatial resolution remotely sensed imagery (IKONOS). *Systematics and Biodiversity* 2:113-119.

Gao, J., 1999. A comparative study on spatial and spectral resolutions of satellite data in mapping mangrove forests. *Int. J. Remote Sens*. 20:2823-2833.

Green, E.P., Clark, C.D., Munby P.J., Edwards A.J. and Ellis, A.C. 1998. Remote Sensing thechniques for mangrove mapping. *Int. J. Remote Sens*. 19:935-956.

Ketterings, Q.M., Coe, R., van Noordwijk, M., Ambagau, Y. and Palm, C.A. 2001. Reducing uncertainty in the use of allometric biomass equations for predicting above-ground tree biomass in mixed secondary forests. *Forest Ecol. Manag.*

146:199-209.

Komiyama, A., Jintana, V., Sangtiean, T. and Kato, S. 2002. A common allometric equation for predicting stem weight of mangroves growing in secondary forests. *Ecol. Res.* 17: 415-418.

Rodriguez, W. and Feller, I.C. 2004. Mangrove landscape characterization and change in Twin Cays, Belize using aerial photography and IKONOS satellite data. *Atoll Res. Bulletin* 513:1-22.

Saito, H., Bellan, M.F., Al-Habshi, A., Aizpuru, M. and Blasco, F. 2003. Mangrove research and coastal studies with SPOT-4 HRVIR and TERRA ASTER in the Arabian Gulf. *Int. J. Remote Sens.* 24:4073-4092.

Wang, L., Sousa, W.P. and Gong, P. 2004a. Integration of object-based and pixel-based classification for mapping mangroves with IKONOS imagery. *Int. J. Remote Sens.* 25: 5655-5668.

Wang, L., Soura, W.P., Gong, P. and Biging, G.S. 2004b. Comparison of IKONOS and QuickBird images for mapping mangrove species on the Caribbean coast of Panama. *Remote Sens. Environ*. 91:432-440.

Wang, L., Gong, P. and Biging, S. 2004c. Individual tree-crown delineation and treetop detection in high-resolution aerial imagery. *PE & RS* 70:351-357.

ASSESSING BIOMASS IN *EUCALYPTUS GLOBULUS* PLANTATIONS IN GALICIA USING DIFFERENT LIDAR SAMPLING DENSITIES

Eduardo GONZÁLEZ-FERREIRO[a], Ulises DIÉGUEZ-ARANDA[a], Luis GONÇALVES-SECO[b], Rafael CRECENTE[a], David MIRANDA[a]

[a] Department of Agroforestry Engineering, University of Santiago de Compostela. R/ Benigno Ledo, Campus universitario, 27002 Lugo, Spain, Phone: 00 34 982 823 259, e-mail: edu.g.ferreiro@gmail.com, ulises.dieguez@usc.es, rafael.crecente@usc.es, david.miranda@usc.es.

[b] CICGE – Department of Applied Mathematics, University of Porto. R/ Campo Alegre, 687, 4169-007, Porto, Portugal. Phone: 00 351 220 402 272, e-mail: lgs@fc.up.pt.

ABSTRACT

The continued growth in energy demand in technologically developed societies makes it necessary to diversify the means of energy production. The region of Galicia (NW Spain), offers great potential for forest production, with an average standing timber volume of 95 $m^3\ ha^{-1}$, higher than Finland's and equivalent to the average standing timber volume reported for Sweden (Bermúdez and Touza, 2000). Furthermore, Galician *Eucalyptus globulus* Labill. (Tasmanian Blue Gum) plantations are internationally renowned for their high timber growth, with an average between 7 and 30 $m^3\ ha^{-1}\ yr^{-1}$, reaching up to 50 $m^3\ ha^{-1}\ yr^{-1}$ in the best sites (Riesco, 2007). Therefore, the possibility of exploiting forest biomass of the high density *Eucalyptus globulus* plantations provides a good opportunity to improve economic performance in forestry, because *Eucalyptus globulus* stands which lack proper management often provide small and low-quality wood which could be used for energy production.

In Galicia there are important deficiencies in the characterization and quantification of the biomass resource available. Conventional methods for biomass estimation are based on field measurements and, although these methods are more direct, they are generally limited in terms of spatial and temporal samplings since they require time-consuming destructive sampling (García et al., 2010). The lack of specific inventories, means results have to be obtained from data sources and existing cartographic sources, which often provide inaccurate information. Remote sensing provides the only method for generating detailed and spatially explicit information on forest biomass, given its potential to provide information at a wide range of spatial and temporal scales (García et al., 2010). LiDAR (*Light Detection and Ranging*) flights can provide a direct assessment of vertical forest structure (Wagner et al., 2008).

Probably the most widely used method for deriving forest variables at stand level, particularly mean height, volume and basal area, is a statistically-based method that uses allometric models fitted to metrics of the LiDAR-derived distribution of canopy heights and field data of experimental plots. This method has shown promising results in forest measurements, even at very low sampling densities of about 1 pulse m^{-2} (Næsset, 2002; Næsset, 2004), which makes it very interesting for commercial operation.

This study aims to estimate biomass fractions of *Eucalyptus globulus* plantations using height and intensity data from a discrete-return LiDAR system, given the importance of the species in the Galician forestry industry and the potential of the method for reducing data acquisition costs. The particular goals are: (1) To prove the applicability of linear, allometric and exponential models to predict biomass in different aboveground fractions; (2) To evaluate the usefulness of intensity data recorded by small footprint systems to estimate biomass; (3) To assess the effect of point density on the estimation of biomass fractions, considering data availability, since the Spanish National Geographic Institute will soon release low-density LiDAR data (0.5 pulses m^{-2}) for the whole of Spain. The equations developed by us will allow estimation of biomass stocks for large areas of *Eucalyptus globulus* rather than using scarce field plot measurements, taking into account the forthcoming availability of LiDAR data for Spain.

The study area was located in Galicia and covered 4 km^2 of high density *Eucalyptus globulus* plantations. LiDAR data was acquired in November 2004 using an Optech ALTM 2033 sensor. First and last return pulses were registered with an average measuring density of about 4 pulses m^{-2}. Fieldwork was carried out between February and March 2005. A forest inventory of 39 square plots of 15 m^2 was conducted in mature *Eucalyptus globulus* plantations. Topographic surveys were conducted to determine the location of the corners of the plots. For all the trees within the plots, total height and diameter was measured.

The fractions of biomass were calculated for each single tree from the following equations (Diéguez-Aranda et al., 2009, p. 238):

$$w_w + w_{b7} = 0.01308 \ d^{1.870} h^{1.172}$$

$$w_b = 0.01010 \ d^{2.484}$$

$$w_{b2-7} + w_{b0.5-2} = 0.003685 \ d^{2.654}$$

$$w_{b0.5} = 0.01258 \ d^{1.705}$$

$$w_l = 0.02949 \ d^{1.917}$$

where w_w is stem wood biomass (kg), w_{b7} is wood and bark biomass on branches with 7 cm minimum top diameter (kg), w_b is bark biomass on stem (kg), w_{b2-7} is wood and bark biomass on branches with 7 cm maximum butt diameter and 2 cm minimum top diameter (kg), $w_{b0.5-2}$ is wood and bark biomass on branches with 2 cm maximum butt diameter and 0.5 cm minimum top diameter (kg), $w_{b0.5}$ is wood and bark biomass on branches with 0.5 cm maximum butt diameter (kg), w_l is leaf biomass (kg), d is diameter at breast height outside bark (1.3 m above ground level, cm), and h is total tree height (m).

Finally, crown biomass (w_{cr}), stem biomass (w_{st}) and aboveground biomass (w_{abg}) were calculated from the sum of the fractions of biomass included:

$$w_{cr} = w_{b2-7} + w_{b0.5-2} + w_{b0.5} + w_l$$

$$w_{st} = w_w + w_{b7} + w_b$$

$$w_{abg} = w_{cr} + w_{st}$$

The fractions of biomass obtained were used to estimate the following variables at the plot level: crown biomass (W_{cr}, kg ha^{-1}), stem biomass (W_{st}, kg ha^{-1}) and aboveground biomass (W_{abg}, kg ha^{-1}). Such estimates were used to develop models to derive biomass fractions at stand level from LiDAR data.

In order to know how LiDAR density affects the precision of biomass estimates, a random reduction of LiDAR returns was performed and a thinned dataset with a density of 0.5 pulses m^{-2} was obtained. For both data sets (original and thinned) intensity data was normalized to a user-defined standard range, eliminating the effect of path length variations on the intensity recorded by the system (Donoghue et al., 2007; García et al., 2010)

For the two datasets, a set of metrics were calculated for pulse intensity and height values of LiDAR data collected within the limits of field plots. These metrics were used as independent variables in the regression models. Linear, allometric and exponential models were used to establish empirical relationships between field measurements and LiDAR measurements. Their general expressions are as follows:

$$Y = \beta_0 + \beta_1 X_1 + \beta_2 X_2 + \ldots + \beta_n X_n$$
$$Y = \beta_0 X_1^{\beta_1} X_2^{\beta_2} \ldots X_n^{\beta_n}$$
$$Y = \exp(\beta_0 + \beta_1 X_1 + \beta_2 X_2 + \ldots + \beta_n X_n)$$

where Y are field values of W_{cr} (kg ha^{-1}), W_{st} (kg ha^{-1}) and W_{abg} (kg ha^{-1}), and X_1, X_2…, X_n may be any of the following LiDAR metrics: h_{mean}, h_{max} and h_{min} are the mean, maximum and minimum heights of LiDAR returns for each plot (m); h_{median}, h_{mode}, h_{SD} and h_{AAD} are the median, mode, standard deviation and average absolute deviation of the height distribution of laser returns for each plot (m); h_{ID} is the interquartile range (m); h_v is the variance of the height distribution of returns for each plot (m^2); h_{Skw} and h_{Kurt} are the coefficients of skewness and kurtosis for height distributions; h_{05}, h_{10}, h_{20}…, h_{90}, h_{95} are the percentiles of LiDAR height distribution for each plot (m); h_{25} and h_{75} are the first and third quartiles of height distribution (m); i_{mean}, i_{max} and i_{min} are the mean, maximum and minimum intensities of LiDAR returns for each plot; i_{median}, i_{mode}, i_{SD} and i_{AAD} are the median, mode, standard deviation and average absolute deviation of the distribution of pulse intensities for each plot; i_{ID} is the interquartile range; i_v is the variance of the distribution of pulse intensities for each plot; i_{Skw} and i_{Kurt} are the coefficients of skewness and kurtosis of the distribution of pulse intensities; i_{05}, i_{10}, i_{20}…, i_{90}, i_{95} are the percentiles of the distribution of LiDAR pulse intensities for each plot; and i_{25} and i_{75} are the first and third quartiles of intensity distribution; r_2 is the number of returns above 2 m height for each plot; and $c_{2\text{-}FP}$ is the ratio of the number of laser hits above 2 m height to the number of first returns for each plot, expressed as a percentage.

To select the variables and to make an initial estimation of the parameters included in allometric and exponential models, the models were linearized by taking logarithms of both sides of (11) and (12). Stepwise selection was performed to select variables to be included in the final models. No predictor variable was left in the model with a partial F-statistic with a significance level greater than .05. The standard least-squares method was used. The analysis of the goodness of fit of the models was based on numerical and graphical comparisons of residuals. For this purpose, the coefficient of determination (R^2) and the root mean square error (RMSE) were used. Besides, a visual inspection of the graphs of residuals against the predicted values of each fitted model was performed. To check for multicollinearity among the explanatory variables of the analyzed models, the condition index (CI) was used. According to Belsley (1991, p. 139-141), regressors with a condition index above 30 were not included in the models.

The goodness-of-fit statistics of the different models tested are presented in table 1. Exponential models provided very stable results after reducing sampling density, with differences between 0.64 and 1.95% in terms of R^2, while allometric models were the least stable with differences between 9.54 and 11.61% in terms of R^2. None of the regression models finally selected included as independent variables related to the intensity of the returns. Exponential models performed best for all the variables, using both full density data and thinned data. Results of biomass estimation suggest that laser pulse density can be reduced for forest purposes to low densities (of up to 0.5 pulses m^{-2}) without significant loss of information.

Table 1. Goodness of fit statistics of the different models tested for stand biomass estimation.

Dependent Variable	Pulses m^{-2}	Model	Independent Variable	R^2	RMSE (kg ha^{-1})	CI
W_{cr}	0.5	Linear	h_{90}	0.708	3812	13.3
	0.5	Allometric	h_{60}	0.619	4882	28.9
	0.5	Exponential	h_{75}	0.755	3771	11.9
	4	Linear	h_{75}	0.719	3736	12.0
	4	Allometric	h_{60}	0.700	4261	29.5
	4	Exponential	h_{75}	0.770	3555	12.0
W_{st}	0.5	Linear	h_{75}, h_{Skw}	0.801	24732	14.3
	0.5	Allometric	h_{60}	0.740	32622	28.9
	0.5	Exponential	h_{75}	0.853	22129	11.9
	4	Linear	h_{75}	0.803	24261	12.0
	4	Allometric	h_{60}	0.818	26139	29.5
	4	Exponential	h_{75}	0.859	21229	12.0
W_{abg}	0.5	Linear	h_{95}	0.771	29453	12.9
	0.5	Allometric	h_{60}	0.727	37347	28.9
	0.5	Exponential	h_{75}	0.844	25668	11.9
	4	Linear	h_{75}	0.797	27723	12.0
	4	Allometric	h_{60}	0.806	30281	29.5
	4	Exponential	h_{75}	0.851	24416	12.0

In the light of the results of this study, the low-density LiDAR data (0.5 pulses m^{-2}) that will soon be released by the Spanish National Geographic Institute will be an excellent source of information for aboveground biomass estimation.

Keywords: Intensity, Biomass fraction, Area-based inventory, Galician forestry, Blue gum eucalyptus.

ACKNOWLEDGMENTS

I want to thank César Cruzado-Campo for his assistance regarding the estimation of biomass stocks. Also I want to thank Laura Barreiro-Fernández, Sandra Buján-Seoane, Dorinda Sarmiento and Marcos Boullón for their invaluable help. This work was supported, in part, through the *Dirección Xeral de Investigación, Desenvolvemento e Innovacción (Xunta de Galicia)* and its fellowship schedule *María Barbeito.*

REFERENCES

Belsley, D. 1991. *Conditioning diagnostics: collinearity and weak data in regression*. New York.

Bermúdez, J. and Touza, M. 2000. Las cifras del tercer inventario forestal en Galicia y su incidencia en la industria de transformación de la madera. *Revista CIS-Madera*. 4: 6-24.

Diéguez–Aranda, U., Rojo Alboreca, A., Castedo–Dorado, F., Álvarez González, J. G., Barrio–Anta, M., Crecente–Campo, F., González González, J. M., Pérez–Cruzado, C., Rodríguez Soalleiro, R., López–Sánchez, C. A., Balboa–Murias, M. A., Gorgoso Varela, J. J. and Sánchez Rodríguez, F. 2009. *Herramientas selvícolas para la gestión forestal sostenible en Galicia*. Xunta de Galicia. Santiago de Compostela.

Donoghue, D., Watt, P., Cox, N. and Wilson, J. 2007. Remote sensing of species mixtures in conifer plantations using LiDAR height and intensity data. *Remote Sensing of Environment*. 110: 509-522.

García, M., Riaño, D., Chuvieco, E. and Danson, F. 2010. Estimating biomass carbon stocks for a Mediterranean forest in central Spain using LiDAR height and intensity data. *Remote Sensing of Environment*. 114: 816-830.

Næsset, E. 2002. Predicting forest stand characteristics with airborne scanning laser using a practical two-stage procedure and field data. *Remote Sensing of Environment.* 80: 88-99.

Næsset, E. 2004. Practical large-scale forest stand inventory using a small-footprint airborne scanning laser. *Scandinavian Journal of Forest Research*. 19: 164-179.

Riesco, G. 2007. Aspectos particulares de la ordenación de plantaciones de eucalipto (*Eucalyptus globulus Labill.*). *In the II Simposio Iberoamericano de Eucalyptus globulus*, 17-20 October 2006, Pontevedra, Spain, pp. 171–180.

Wagner, W., Hollaus, M., Briese, C. and Ducic, V. 2008. 3D vegetation mapping using small-footprint full-waveform airborne laser scanners. *International Journal of Remote Sensing*, 29: 1433-1452.

BIOMASS ESTIMATES BY SATELLITE DATA AND GROUND MEASUREMENTS

Gherardo CHIRICI[a], Piermaria CORONA[b], Marco MARCHETTI[a], Daniela TONTI[a], Davide TRAVAGLINI[c]

[a] University of Molise, Contrada Fonte Lappone – 86090 Pesche, Isernia, Italy. Phone +39-0874-404138, Fax +39-0874-404123, e-mail: gherardo.chirici@unimol.it
[b] University of Tuscia, Via S. Camillo de Lellis – 01100 Viterbo, Italy. Phone +39-0761-357425, Fax +39-0761-357389, e-mail: piermaria.corona@unitus.it
[c] University of Florence, Via S. Bonaventura, 13 – 50145 Florence, Italy. Phone +39-055-3288618, Fax +39-055-319179, e-mail: davide.travaglini@unifi.it

ABSTRACT

Forest ecosystems are the world's largest accessible source of biomass, and their use for energy purposes is part of the international political and economical debate (Parika, 2004). In 2005 in Italy forest harvesting was close to 10 Mm^3, and more than 60% was firewood, largely from coppice stands. Coppice stands cover in Italy 36,631 km^2 on a total forested area of 104,675 km^2 and on a total land area of 301,328 km^2 (INFC, 2005).

The main source of information for the estimation of forest resources are National Forest Inventories (NFIs) (McRoberts et al., 2009). NFIs are able to provide information aggregated for large geographical regions inferring from information acquired in the field in sampling units geographically distributed on the basis of a formally defined sampling design.

Biomass estimates are relevant for many ecological studies and issues related to global change. For example, they can be used in models to assess the contribution of forest fires to the increase in atmospheric carbon dioxide concentration. Biomass assessment by field observations has been found insufficient to present spatial variability of biomass over large area. Satellite remote sensing data provide capability for biomass mapping (e.g., Labreque et al., 2006; Blackard et al., 2008).

One of the most promising methodology to carry our such spatial estimations is *k*-Nearest Neighbors (*k*-NN) that is able to produce locally calibrated estimates for individual satellite image pixels and continuous maps of forest attributes using data sampled in the field (Mcroberts and Tomppo, 2007; McRoberts, 2008). The application of the *k*-NN method was proved to be useful in providing local estimates of forest fuel potentials in the boreal area (Bååth et al., 2002). No studies were developed to test such an approach in Mediterranean conditions when firewood is obtained from broadleaves forests managed with the coppice system.

The aim of this paper is the aboveground biomass *k*-NN estimation of forests, pastures and meadows in Molise Region, central Italy.
The study area is 443,700 ha wide. For the study area the following information were available. A vegetation maps developed by manual interpretation of high resolution aerial orthophotos and field work. The map has a thematic accuracy of at least 85% and

was developed with a reference nominal scale of 1:10.000 and a minimum mapping unit of 0.5 ha (Garfì and Marchetti, 2010). In this study the map was reclassified in order to derive a boolean mask covering forests, pastures and meadows. This target area is 165,000 ha wide.

A local forest inventory was developed on the basis of an unaligned systematic sampling design. For each sampling unit (a 15 m radius circle) the aboveground tree biomass was calculated from growing stock volume trough expansion factors. Grass and shrub biomass were measured with destructive approach in squared subplots 1 m width, four subplots for each plot. For this study a total of 181 geolocated plots with the total aboveground biomass were available.

Three different remotely sensed data were available for this study: one Landsat 5 TM (30 m resolution) scene acquired in August 2006, one IRS P6 LISS III (20 m resolution) scene acquired in July 2006, and a SPOT 5 HRG (10 m resolution) coverage acquired in August 2006. All the images were orthocorrected and coregistered in the same geographic projection.

For each one of the 181 sampling units the spectral signature of all the bands for all the available images was extracted. The *k*-Nearest Neighbors (*k*-NN) non parametric estimation method was applied on the basis of a leave-one-out (LOO) procedure for each one of the 181 sampling units. Several *k*-NN configurations were tested on the basis of different multidimensional distance measures (Euclidean distance, Mahalanobis distance, distance weighted with fuzzy weights) and different *k* values (Chirici et al., 2008). For each test trough LOO the accuracy of the *k*-NN estimations was calculated in terms of R^2 and Root Mean Square Error (RMSE). The locally best configuration was finally defined and applied for each pixel of the target mask.

During the LOO phase (Figure 1) the best k-NN configuration was defined (IRS imagery, fuzzy distance, *k*=6). This configuration was applied in order to estimate for each IRS pixel in the target mask the total aboveground biomass of forests, pastures and meadows in the study area (Figure 2). The percentual RMSE of the final map was equal to 5%.

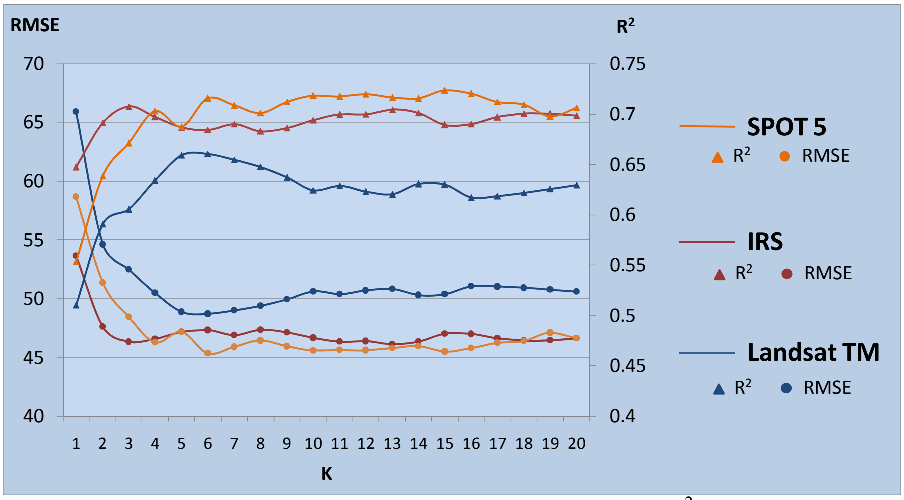

Figure 1. Accuracy evaluation of *k*-NN biomass estimation (in terms of R^2 and RMSE) based on leave-one-out cross for different *k* values and for the three different types of remotely sensed data.

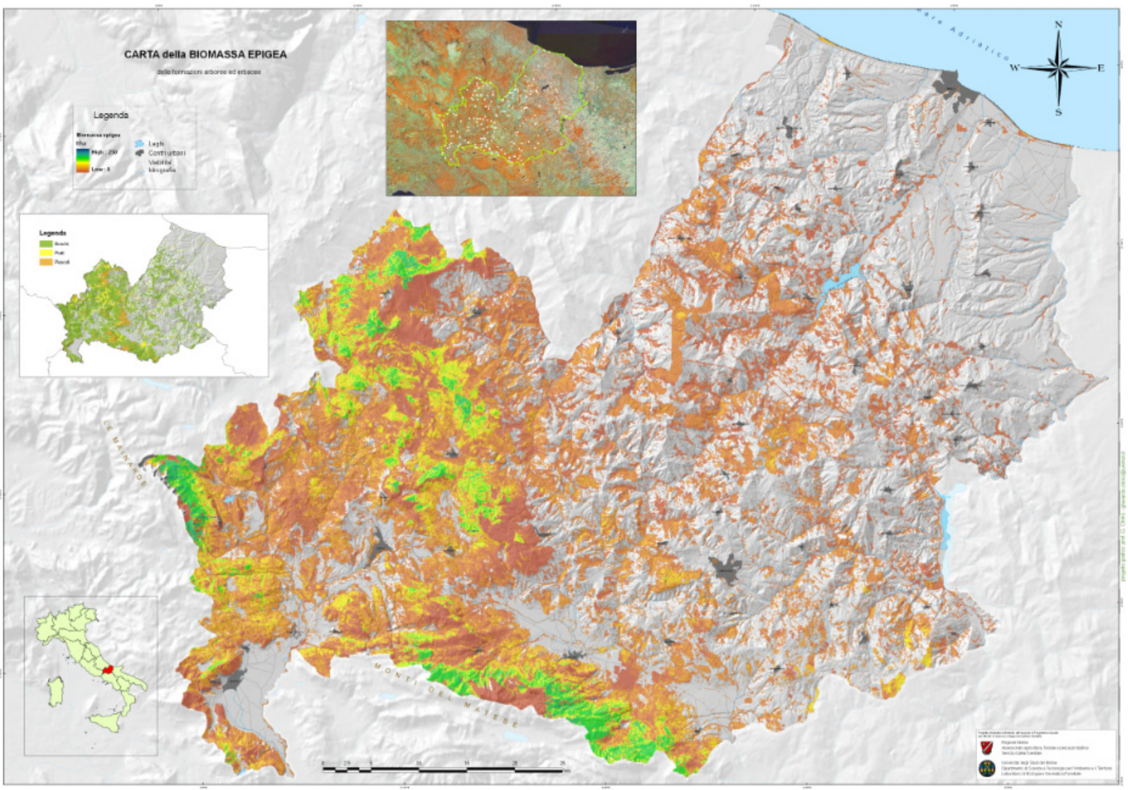

Figure 2. Biomass map created by *k*-NN over the study area. In the top frame the location of the sampling units, in the left frame the forest and pasture mask, and in the bottom frame the location of the study area in Italy.

Keywords: biomass; forest inventory; satellite image; *k*-Nearest Neighbours, estimation.

REFERENCES

Bååth, H., Gällerspång, A., Hallsby, G., Lundström, A., Löfgren, P., Nilsson, M. and Ståhl, G. 2002. Remote sensing, field survey, and long-term forecasting: an efficient combination for local assessments of forest fuels. *Biomass and Bioenergy* 22(3): 145-157.

Blackard, J.A., Finco, M.V., Helmer, E.H., Holden, G.R., Hoppus, M.L., Jacobs, D.M., Lister, A.J., Moisen, G.G., Nelson, M.D., Riemann, R., Ruefenacht, B., Salajanu, D., Weyermann, D.L, Winterberger, K.C., Brandeis, T.J., Czaplewski, R.L., McRoberts, R.E., Patterson, P.L. and Tymcio, R.P. 2008. Mapping U.S. forest biomass using nationwide forest inventory data and moderate resolution information. *Remote Sensing of Environment* 112: 1658–1677.

Chirici, G., Barbati, A., Corona, P., Marchetti, M., Travaglini, D., Maselli, F. and Bertini, R. 2008. Non-parametric and parametric methods using satellite imagery for estimating growing stock volume in alpine and Mediterranean forest ecosystems, *Remote Sensing of Environment* 112: 2686–2700.

Garfi, V. and Marchetti, M. 2010. Tipologie forestali e preforestali della regione Molise. Edizioni dell'Orso, Alessandria.

INFC, 2005. Inventario nazionale delle foreste e dei serbatoi forestali di carbonio. Ministero delle Politiche Agricole Alimentari e Forestali, Ispettorato Generale - Corpo Forestale dello Stato. CRA - Istituto Sperimentale per l'Assestamento Forestale e per l'Alpicoltura; 2005. Estensione delle macrocategorie inventariale Bosco e Altre terre boscate, ripartite per tipi colturali. Available at http://www.sian.it/inventarioforestale/doc/dati/cap_09_tipocolturale/09_t9.1_9.2.pdf.

Labrecque, S., Fournier, R.A., Luther, J.E. and Piercey, D. 2006. A comparison of four methods to map biomass from Landsat-TM and inventory data in western Newfoundland. *Forest Ecology and Management* 226: 129–144.

McRoberts, R.E. 2008. Using satellite imagery and the k-nearest neighbors technique as a bridge between strategic and management forest inventories. *Remote Sensing of Environment* 112: 2212-2221.

McRoberts, R.E. and Tomppo, E.O. 2007. Remote sensing support for national forest inventories. *Remote Sensing of Environment* 110: 412-419.

McRoberts, R.E., Tomppo, E., Schadauer, K., Vidal, C., Stahl, G., Chirici, G., Lanz, A., Cienciala, E., Winter, S., Smith, B. 2009. Harmonizing National Forest Inventories. *Journal of Forestry*: 179-187.

Parika, M. 2004. Global biomass fuel resources, *Biomass and Bioenergy* 27: 613-620.

KNOWLEDGE-BASED CLASSIFICATION OF VERY HIGH SPATIAL RESOLUTION REMOTE SENSING DATA FOR A MODEL OF ORGANIC CARBON STOCKS IN RIPARIAN FOREST SOILS

Leonhard SUCHENWIRTH[a], Michael FÖRSTER[a]

[a]Technische Universität Berlin, Institute of Landscape Architecture and Environmental Planning, Department of Geoinformation Processing, Office EB 5, Straße des 17. Juni 145, 10623 Berlin,
e-mail: leonhard.suchenwirth@tu-berlin.de, michael.foerster@tu-berlin.de

ABSTRACT

The intention of this paper is to present the derivation of forestry-specific vegetation parameters from Very High Spatial Resolution (VHSR) Remote Sensing Data and auxiliary geodata for a knowledge-based model of organic carbon stocks in floodplain soils.

Floodplain soils play a crucial role for the storage of organic carbon; however there are few data available on carbon stocks in these soils compared to other terrestrial ecosystems. Even though remote sensing data have been used for the detection of soil characteristics for quite some time (McBratney et al., 2003), there is still no scientific basis for the generation of large scale soil maps that show the distribution of organic carbon stocks in floodplain soils.

The research area is the Donauauen (Danube Floodplains) National Park, which is situated along the river Danube between Vienna, Austria and Bratislava, Slovakia. It preserves one of the last remaining major wetlands environment in Central Europe. Here, the Danube is still free flowing and is the lifeline of the National Park.

In a first approach (Cierjacks et al., 2010) the variables water regime, the vegetation, the relief position and the content of clay and iron oxides were identified to have an effect on the carbon content (see Figure 1). Two different types of sedimentation areas can be distinguished: a) Dynamic areas, stocked with younger trees and a higher number of trees, and due to frequent inundations with a high flow velocity a higher number of soil horizons; and b) stable areas with a lower number of trees, a higher distance to the river, and due to a lower flow velocity during inundations a lower number of soil horizons. On aerial images, five woodland types could be differentiated visually: *Salix alba, softwood floodplain forests, populus alba, populus x canadensis and hardwood floodplain forests.*

Based on these findings the overall goal is to develop a knowledge-based method of remote sensing to model the spatial distribution of organic carbon stocks in floodplain soils, using very high resolution remote sensing data and auxiliary data. This method should support large-scale mapping of organic carbon stocks in floodplain soils. Knowledge from soil science can be regionalised and be used for the increased demands of landscape and environmental mapping, especially regarding the climate function of soils.

The methodology is based on spectral and knowledge-based classification. In order to determine vegetation parameters, such as vegetation type, age, density of trees per hectare, a combination of pixel and object-based classifications is used. Object-based image analysis has been used frequently in the recent years for the classification of very high resolution remote sensing imagery (Kubo et al., 2005, Kubo et al., 2007, Chubey et al., 2006).

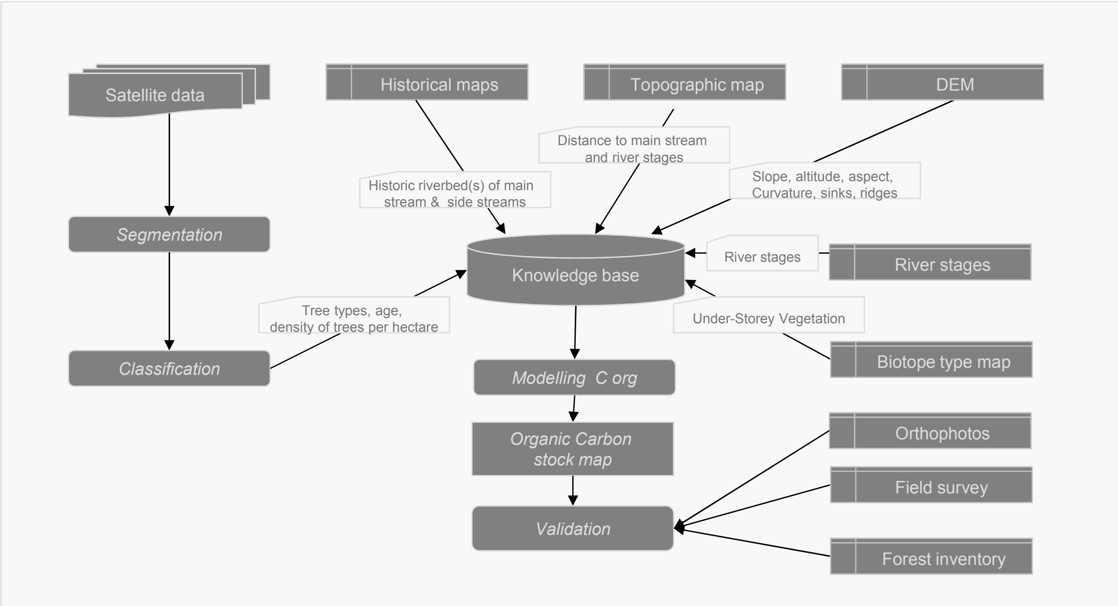

Figure 1. Model of organic carbon stocks in floodplain soils, influenced by various data sources and derived parameters.

For this study an Ikonos scene from April 2009, and a digital terrain and surface model, based on an airborne Laser scanning, with a resolution 2.5 meters were utilized; besides, there are recent and historic maps that show the course of the main river current. Other additional data-sources include the forest inventory, field survey data, as well as biotope type maps.

So far, a classification of vegetation types has been made, based on image objects gained by segmentation. Besides spectral values of the IKONOS satellite image, texture values as well as the digital terrain model were used for the delineation of vegetation classes. For instance, the altitude above sea level can determine whether a forest is classified as softwood or hardwood forest, similarly the distance to the main stream of the river Danube have an influence on the classification.

These results will be integrated into a rule-based classification process, using fuzzy logic to integrate additional data and expert knowledge into the spectral classification. The influence of the different parameters shall be explained by statistical methods, such as multiple linear regression.

Keywords: Floodplain soils, carbon stocks, Ikonos, Object-based image analysis.

ACKNOWLEDGMENTS

The authors want to thank the German research Foundation (DFG) for the funding of this project, as well as the Donauauen National Park administration for the provision of geodata.

REFERENCES

Chubey, M.S., S.E. Franklin, and M.A. Wulder, 2006, Object-based Analysis of Ikonos-2 Imagery for Extraction of Forest Inventory Parameters. Photogrammetric Engineering & Remote Sensing, Vol. 72, No. 4, pp. 383-394.

Cierjacks A, Kleinschmit B, Babinsky M, Kleinschroth F,Markert A,Menzel M, Ziechmann U, Schiller T, Graf M, Lang F. 2010. Carbon stocks of soil and vegetation on Danubian floodplains. *Journal of Plant Nutrition and Soil Science*

IPCC, 2000, Special Report on Land Use, Land-Use Change and Forestry. Cambridge University Press, Cambridge, UK, p.24.

Kubo, M. and Muramoto, K., 2005, Tree crown detection and classification using forest imagery by IKONOS, Proceedings of IGARSS, vol.6, pp.4358-4361.

Kubo, M., Nishikawa, S., E. Yamamoto, and K. Muramoto, 2007, Identification of individual tree crowns from satellite image and image-to-map rectification, 1905-1908.

McBratney, A.B., M.L. Mendonca Santos and B. Minansy 2003, On digital soil mapping.7 *Geoderma* 117 pp. 3–52.

MAPPING THE BIOMASS OF GOLA FOREST RESERVE IN SIERRA LEONE WITH REMOTE SENSING DATA AND NEURAL NETWORKS

Gaia VAGLIO LAURIN[a], Qi CHEN[b], David COOMES[c], Fabio DEL FRATE[a], Giorgio Antonino LICCIARDI[a], Jeremy LINDSELL[d]

[a] Tor Vergata University, Dipartimento di Informatica, Sistemi e Produzione, Via del Politecnico 1, 00133 Rome, Italy, e-mail: laurin@disp.uniroma2.it
[b] Department of Geography, University of Hawai`i at Mānoa, 422 Saunders Hall, 2424 Maile Way, Honolulu, HI, 96822, USA, e-mail: qichen@hawaii.edu
[c] Department of Plant Sciences, University of Cambridge, Downing Street, Cambridge CB2 3EA, United Kingdom, e-mail: dac18@cam.ac.uk
[d] The Royal Society for the Protection of Birds, The Lodge, Sandy, Beds. SG19 2DL, UK, e-mail: Jeremy.Lindsell@rspb.org.uk

ABSTRACT

This work describes the estimation of the above ground live biomass (AGLB) of a tropical forest area, the Gola Forest Reserve in Sierra Leone, from field plot measurements and Landsat TM/ETM+ images, using machine learning techniques for retrieval, and correlating the results with lidar derived metrics from the Geoscience Laser Altimeter System (GLAS) instrument onboard the NASA ICESat satellite.

The study will also contribute to a research modeling effort, supported by the Cambridge Conservation Initiative, aimed at comparing alternative predictive models for carbon emission reductions calculation in the framework of the UN-REDD (United Nations Reduction in Emission from Deforestation and Forest Degradation in Developing Countries) program. Mapping and monitoring carbon stocks and forest changes in tropical regions are essential steps in the implementation of a future carbon market. While accounting methods are still under discussion, efforts are needed to test different carbon monitoring approaches. Selected methods should be efficient, cost-effective and robust enough to enable countries to measure their stock at different scales, from national to local; the former for reporting and accounting purposes and the latter to allow internal forest management, planning and evaluation, conservation prioritization, and to identify the contribution from different areas to the national carbon budget.

The study site (Fig. 1), the Gola Forest Reserve, is the newest National Park in the country with an area of about 710 square km, and the largest closed canopy lowland rain forest remaining in Sierra Leone. The forest holds several endangered species and is a biodiversity hotspot. Due to its protected status and effective conservation work, the Gola forest has been largely undisturbed during the last 10 years.

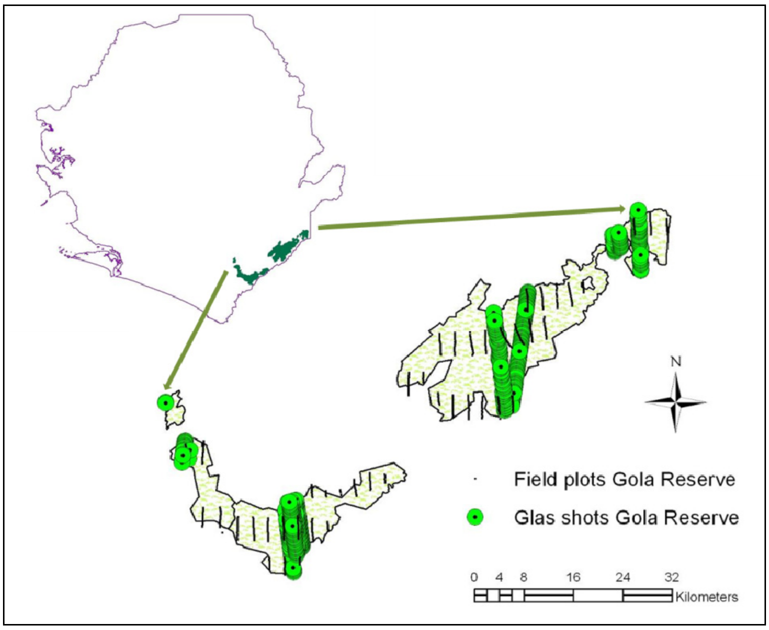

Figure 1. The Gola Reserve study site in Sierra Leone, with location of field plots and GLAS lidar shots

In the reserve, a large number of geographically referenced field plots *(> 700*) were surveyed between January 2006 and March 2007, with AGLB values derived from field measurement using allometric equations according to Chave et al. (2005). Field derived AGLB data were used in part for neural networks training and in part for results validation.

Neural networks already demonstrated well suited for biomass retrieval with optical or radar satellite data (Foody et al. 2001, Del Frate et al. 2004). In this research, the Stuttgart Neural Network Simulator (SNNS) was used to perform the retrieval and the Scaled Conjugate Gradient (SGC; Moller, 1993) was employed as supervised learning algorithm for feed forward the neural network.

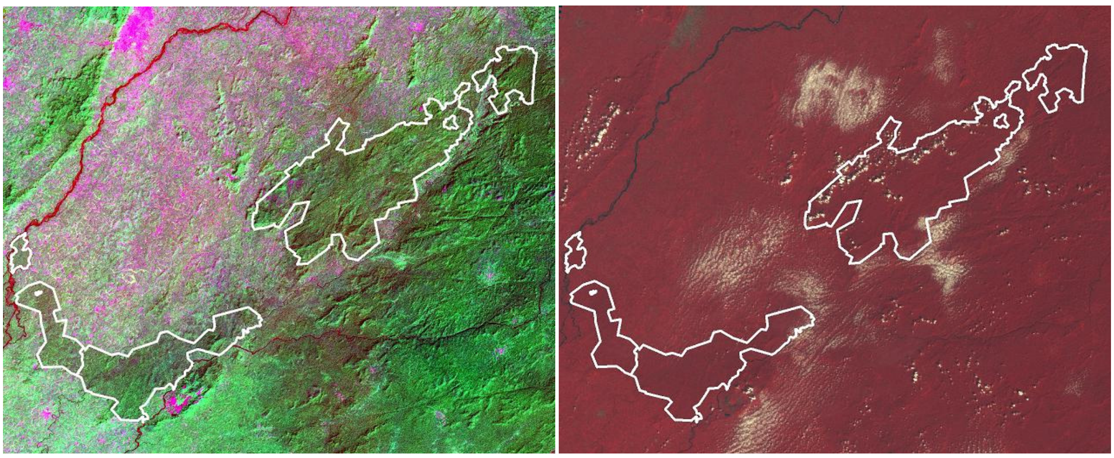

Figure 2. TM Landsat of the Gola Reserve: two false color composites, 5-4-3 dated December 2006 (left) and 4-3-2 dated Jan. 2007 (right).

The study was conducted using only freely available satellite imagery. Four ETM+ and TM Landsat images (Fig. 2) all dated December 2006 or January 2007 were selected, according to their quality, for retrieval purposes. The Landsat imagery was preprocessed and its different steps were employed for network input (raw, calibrated and atmospherically corrected bands). Vegetation indexes were also derived to be used as network inputs. Network training was done with different inputs from images and topologies, also exploring the preprocessing role. The best results were compared to those obtained using traditional regression methods.

About 10.000 GLAS shots dated between 2003 and 2009, also freely available, overlap the field plots in the Gola reserve, while a larger number of footprints are found at distances of 50-100 and 150 meters from the plots. The heterogeneity of Gola Forest in areas of GLAS data availability was explored using Ikonos-2 very high resolution images.

GLAS waveforms might be contaminated by the atmospheric forward scattering or saturated signals. Therefore, only the cloud-free and saturation-free shots were analyzed (Chen, 2010). Different metrics, such as canopy height, height of median energy etc., were extracted from GLAS waveforms and related to biomass values (Fig. 3), to select the most robust ones. ASTER DEM was used to remove the waveform broadening effects over sloped terrain. Results obtained from the Landsat-based retrieval of AGLB were finally correlated with the metrics obtained with different GLAS data.

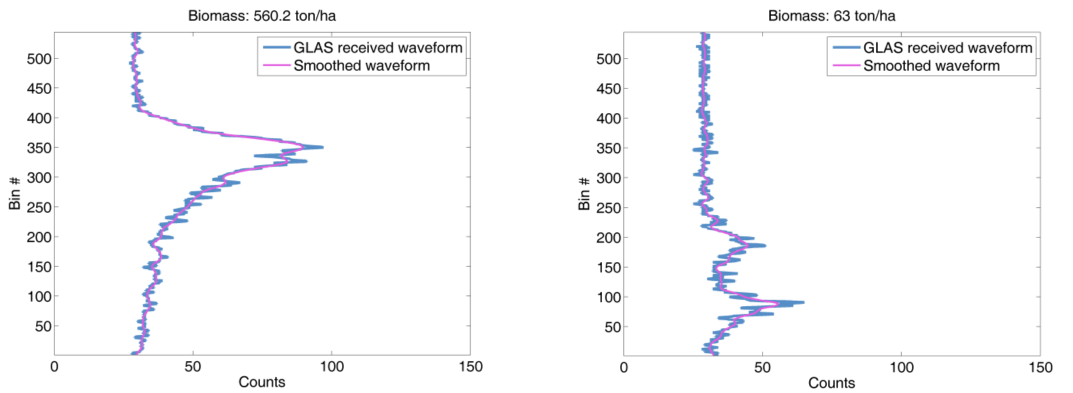

Figure 3. Illustration of using GLAS waveforms for biomass estimation.

To obtain preliminary results, major efforts were needed to screen the ground truth data through visual inspection, in order to produce a field data set corresponding to areas not contaminated by haze, clouds, shadows or other sources of ambiguity.

This screening activity differently reduced the network input dataset for each image, with smaller number of ground truth for ETM+ imagery, already affected by missing data.

Data derived from Landsat ETM+ produced better results than those obtained from TM sensor, as well as those data free from haze contamination or banding artifacts. Preliminary result of regression with neural network and ETM+ Landsat data indicate that predicted results are positively related to field values (r = 0.65). Generalization of the net with input coming from imagery other than those used for net training was unsuccessful, showing that a unique net should be build for each image. The use of atmospherically corrected imagery does not seem to improve the results obtained with calibrated images.

Future already planned efforts include the use of Alos Palsar L-band radar data as additional neural network input and the use of very high resolution optical imagery for forest stratification prior to retrieval in selected reserve sites.

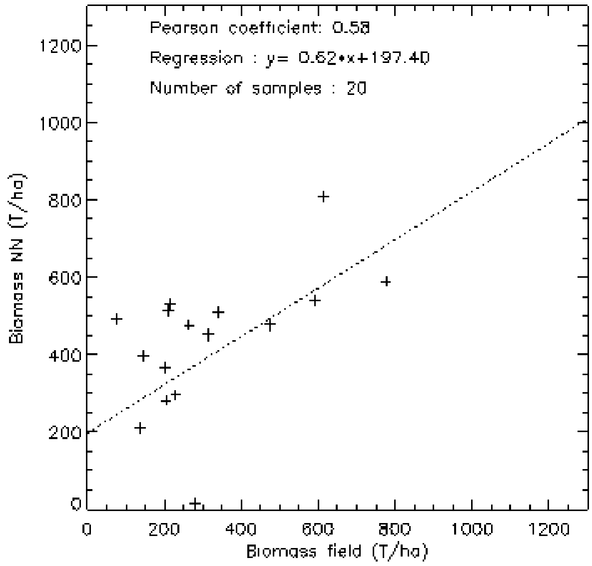

Figure 4. Preliminary results: relationship between field measured biomass and that predicted by SCG neural network (Landsat ETM+ Dec. 2006, *r=0.65*).

Keywords: biomass, neural networks, Landsat, GLAS.

AKNOWLEDGMENTS

Ikonos-2 imagery has been kindly provided by the GeoEye Foundation.

REFERENCES

Chave, J., Andalo C., Brown S., Cairns M. A., Chambers J. Q., Eamus D., Fölster H., Fromard F., Higuchi N., Kira T., Lescure J. -P., Nelson B. W., Ogawa H., Riéra B., Yamakura T. Puig H.et al. 2005. Tree allometry and improved estimation of carbon stocks and balance in tropical forests. *Oecologia* 145:87-99

Chen, Q., 2010. Retrieving canopy height of forests and woodlands over mountainous areas in the Pacific coast region using satellite laser altimetry, *Remote Sensing of Environment*, 114, 1610-1627.

Del Frate, F. and Solimini D. 2004. On neural network algorithms for retrieving forest biomass from SAR data. IEEE Transactions on Geoscience and Remote Sensing, Vol. 42, No. 1

Foody, G. M., Cutler M. E., McMorrow J., Pelz D., Tangki H., Boyd D. S., and Douglas I. 2001 Mapping the biomass of Bornean tropical rain forest from remotely sensed data. *Global Ecology & Biogeography* 10, 379–387.

Moller, M. F. 1993. A scaled conjugate gradient algorithm for fast supervised learning. *Neural Networks*, 6:525--533.

RADIOMETRIC CALIBRATION OF IMAGES FROM DIGITAL PHOTOGRAMMETRIC CAMERAS TO ESTIMATE BIOMASS

Flor ÁLVAREZ[a], Jose-Ramón RODRÍGUEZ-PÉREZ[a], Vicente DEL BLANCO MEDINA[b]

[a] Universidad de León, Campus de Ponferrada, s/n 24400. Ponferrada (Leon, Spain),
e-mail: flor.alvarez@unileon.es, jr.rodriguez@unileon.es
[b] ITACYL. Junta de Castilla y León, Finca Zamadueñas. 47071 (Valladolid, Spain),
e-mail: blamedvi@itacyl.es

ABSTRACT

Estimating and modelling biomass can be helpful for biomass management. It is also interesting to calculate the amount of biomass in a certain area for carbon implications, as indicated by the Kyoto protocol. In the past, remote sensing techniques have been able to estimate biomass by using reflectance in the both the red and the near infrared wavelengths (Rouse et al., 1974 (in: Jensen, 2005); Cho et al., 2007). Nowadays the sensors in the digital photogrammetric cameras gather information not only in the visible wavelengths but also in the near infrared wavelengths, which provides the possibility of using digital photogrammetric data for environmental studies. Nevertheless, there are several weaknesses in current processes that are slowing down the use of radiometric information provided by these sensors. The optimal use of the technological progress requires the calibration and validation of the photogrammetric systems (Honkavaara, 2004). In this context, calibration is the process of defining quantitatively the response of a sensor to a controlled and known input signal (Cramer, 2007).

Flight conditions (i.e. atmospheric conditions, exposure characteristics, solar elevation), and sensor characteristics, as well as post-processing effects (calibration based on radiometric corrections) have an effect on image radiometry (Markelin et al., 2008). As a result, the same object generates different digital numbers depending on its location (in the same image and in different images). Therefore, to use this information in a quantitative approach it is necessary to perform a relative and/or absolute radiometric registration. Moreover, the optimal radiometric processing procedure depends on the final application and the technique selected to extract the information: (i) classic remote sensing (using normalized data from the image) or (i) methods using the characteristics of the anisotropic reflectance of the objects (bidirectional reflectance distribution function) (Honkavaara and Markelin, 2007). Any application related to extracting thematic information requires rigorous processing methods, which are well developed for satellite imagery and airborne sensors, but which are still in development for photogrammetric sensors. The previous issues indicate the need of developing a protocol to process the information in order to be able to use the photogrammetric data to extract thematic data by remote sensing techniques.

A comprehensive review of radiometric aspects of digital photogrammetric images and calibration experiences can be read in Honkavaara et al. (2009).

The National Plan of Aerial Orthophotography (PNOA) updates the photogrammetric information (e.g. orthophotographs) in Spain every two years, but so far none of the

data derived from the photogrammetric flights is used to extract thematic or biophysical information. Therefore it would be interesting to explore the possibility of establishing a relationship between the biomass and the radiometric information captured by the digital photogrammetric cameras, as an added value to the PNOA deliverables. The aim of this research is determining the suitability of the Ultracam Xp and Ultracam Xp for biomass estimation in grasslands.

There are two different study areas in this research. Field A is located in a grassland area in Barakaldo (Bizcaia, Spain). Field B is located in a grassland area in Cogollos (Burgos, Spain). The aerial photograph of Field A was captured by a digital photogrammetric camera Ultracam X with a Ground Sampling Distance (GSD) of 7 cm, while Field B was flown as part of the PNOA with a digital photogrammetric camera Ultracam Xp and a GSD of 25 cm. The images were calibrated to at-surface reflectance using ten portable reflectance targets with nominal reflectance values of 0%, 25%, 50%, 75% and 100%. An empirical line calibration was performed using the reflectance values for the targets and the corresponding Digital Numbers (DNs) in the images.
Twenty 1 m x 1 m sample plots were placed in each study area to validate the biomass estimations obtained from the imagery (Figure 1).

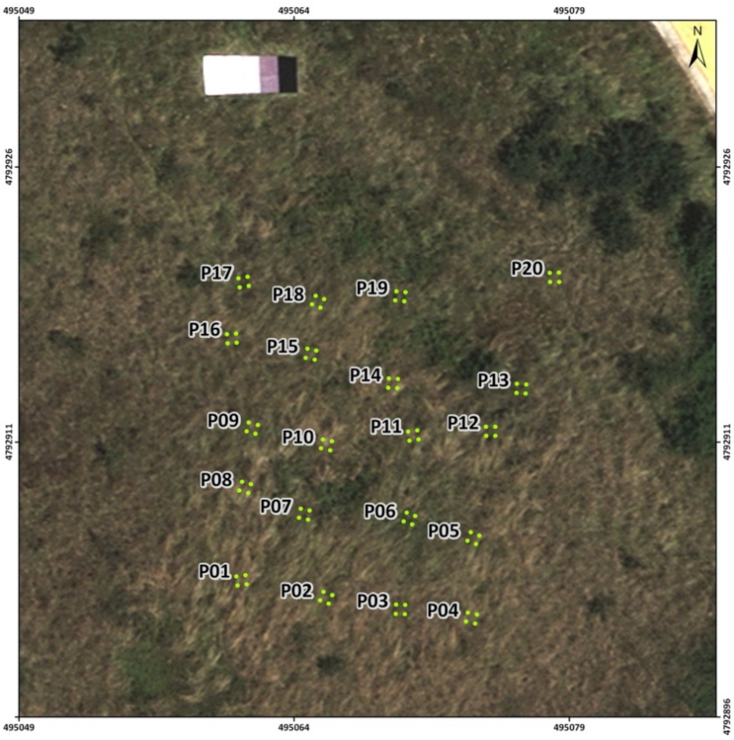

Figure 1. Location of the biomass plots (Pi), sub-plots (in green) and the reflectance targets in the data set A (Barakaldo). Coordinate reference system: ED50 UTM Zone 30.

Each 1 m x 1 m plot was located on a 2 m x 2 m homogeneous area covered by species of the *Gramineae* family. Each plot was then divided into 4 sub-plots (0.50 x 0.50 m). All of the biomass in each sub-plot was harvested and weighed in the field using a portable scale. 10% of the biomass of each NW subplot was stored and kept as a representative sample to determine the plot biomass in the laboratory. The sample was weighed in the laboratory using a precision scale before drying it in an oven. The sample was weighed again using the precision scale after the sample was dried in the oven for 24, 36, and 48 hours at 65ºC, in order to obtain the dried biomass weight at 24 h, 36 h and 48 h. The dried biomass weight was used as surrogate for the aboveground dry biomass in each plot. The data analyses were conducted to study the relationships between the radiometric data gathered by the aerial camera and the biomass estimation. The data was then analyzed by study area and the results of the study areas were compared, in order to study the influence of GSD.

The results showed that it was possible to establish a relationship between the radiometric data gathered by the Ultracam and the dried biomass weight in a grassland area. The vegetation indices NDVI and Simple Ration (SR) were the best predictors for biomass in a grassland area (r^2=0.63 and r^2=0.66, respectively, at a significance level of 5%). The quality of the calibration, as well as the GSD of the image has an impact on the estimation of the dried biomass. It has been shown that three consecutive images gathered with the same camera, during the same flight, and under very similar conditions (data set A) had significant differences in the DNs for the same targets. This means that each image would need a different equation to be radiometrically corrected. In addition, using level 2 imagery instead of level 3 imagery is recommended, so that the original DNs are kept.

Keywords: airborne sensors, near-infrared, thematic, Carbon, forestry, National Plan of Aerial Orthophotography (PNOA).

ACKNOWLEDGMENTS

This research has been partially funded by the Junta de Castilla y León through the project "Calibración radiométrica de cámaras aéreas digitales. Aplicación a la clasificación automática de cubiertas del suelo y estimación de biomasa" (LE001B08).

This research has been developed in collaboration with WIDE WORLD GEOGRAPHIC, S.L. within the project "Calibración radiométrica de imágenes digitales para el control de cambio climático y biomasa en áreas contaminadas o degradadas mediante empleo de la banda infrarroja".

The authors would like to thank Javier Núñez Llamas for all the assistance during the field work and Lucas Martínez for his comments.

The authors would like to thank Bonsai Advanced Technologies for their assistance concerning the use of the spectrometer.

REFERENCES

Cho, M., Skidmore, A., Corsi, F., van Wieren, S. and Sobhan, I. 2007. Estimation of green grass/herb biomass from airborne hyperspectral imagery using spectral indices and partial least squares regression. *Int. J. Appl. Earth Observ. Geoinform*. doi;10.1016/j.jag.2007.2.001.

Cramer, M. 2007. Digital airborne cameras — status and future. *In Proceedings of ISPRS Hannover Workshop 2005: High- Resolution Earth Imaging for Geospatial Information*. 8 p., on CD-ROM.

Honkavaara, E. and Markelin, L. 2007. Radiometric Performance of Digital Image Data Collection - A Comparison of ADS40/DMC/UltraCam and EmergeDSS. *In The Photogrammetric Week 2007*, pp. 117-129 .

Honkavaara, E. 2004. In-flight camera calibration for direct georeferencing. *In The International Archives of Photogrammetry, Remote Sensing and Spatial Information Sciences*, 35, Part B1, pp. 166–171.

Honkavaara E., Arbiol R., Markelin L., Martinez L., Cramer M., Bovet S., Chandelier L., Ilves R., Klonus S., Marshal P., Schläpfer D., Tabor M., Thom C. and Veje N. 2009. Digital Airborne Photogrammetry—A New Tool for Quantitative Remote Sensing?—A State-of-the-Art Review On Radiometric Aspects of Digital Photogrammetric Images. *Remote Sensing* 1(3): 577-605.

Jensen, J.R. 2005. *Digital Image Processing: a Remote Sensing Perspective* (3rd ed.). Prentice Hall, Upper Saddle River, NJ, USA, pp.

Markelin, L., Honkavaara, E., Peltoniemi, J., Ahokas, E., Kuittinen, R., Hyyppä, J., Suomalainen, J., Kukko, A., 2008. Radiometric calibration and characterization of large-format digital photogrammetric sensors in a test field. *Photogramm. Eng. Remote Sens.* 74: 1487-1500.

THE EVALUATION OF DENSITIES OF FOREST MASS EMPLOYING HIGH RESOLUTION DIGITAL IMAGES (QUICKBIRD) THROUGH THE IDENTIFICATION OF LOCAL MAXIMA AT DIGITAL NUMBERS

Eduardo CORBELLE,[a] María Luz GIL[a], Juan ORTIZ[a]

[a] Departamento de Ingeniería Agroforestal, Escuela Politécnica Superior, Campus Universitario s/n, 27002 Lugo – Spain. Phone 982 252231. Fax 982 285926, e-mail: ml.gil@usc.es

ABSTRACT

The present study relates attempts to estimate the density of forest mass employing a high resolution image captured by Quickbird satellite using the technique of detecting local maxima at digital numbers. The study site is located in Lugo - Spain.

We evaluate which variants of the technique are the most recommendable and the reliability of the obtained estimate, given the available image and the characteristics of the masses in the study area. We also analyze the relationship that exists between the estimation error and the type of mass being studied; the latter defined by two parameters: the main arboreal specie and mass density.

The identification of individual trees through the detection of local maxima is a simple application technique which is well documented in bibliography (Leckie et al., 1999a Wulder et al., 2000 and 2004). The efficiency of this detection is usually high and depends, fundamentally, on two characteristics of forest masses: the first is the size of the crown that it's related with the pixel size and the second is the shape of the crown so that the best results correspond with trees with cone-shaped crowns. Other factors such as the angle of solar elevation also influence the results. One of the principal problems with this technique, according to some authors, is the possibility of having a high error of commission (false positives) and this seems to be the case in images with a particularly high resolution (approximately 20 cm pixel size). For images like QuickBird (70 cm / pixel) and in the specific case of estimating mass density, it seems more reasonable to assume a greater weight of error omission which would give rise to a significant tendency to underestimate. Consequently, instead of applying variants of the method directed at reducing the commission error (for example, through increasing the size of the search window or employing low pass filters), this study evaluates variants of the method related to correcting the tendency to underestimate density.

There have been selected 20 experimental units, with an area between 0,22 and 3,18 hectares (mean 1,21 hectares) including hardwood and softwood and including masses of a certain age and reforested ones. Each location was visited and photographed and information was obtained relating to species and density in addition to information on lower level vegetation, approximate age and such.

Figure 1. Shows an example of one experimental unit, identified in the image and as seen on land.

The detection was carried out using the possibilities of the raster calculation of a Geographical Information System by executing the order which compares the digital number of each pixel with the surrounding 8 pixel values (3 pixels×3 pixels window as proposed by Gougeon et al., 2001) assigning value "1" if it is greater than all the others or "0" if it is smaller. The result is a raster file with two possible values: 1 (maximum local) and 0 (the rest) which can be seen in figure 2 (projected on the original image).

Once the detection of local maxima in the image has been achieved it is necessary to know which correspond to the different experimental units. To do this we have a raster file which is codified to differentiate the pixels corresponding to each one of them. Multiplying this file by the result of the detection of local maxima we obtain a new file in which each local maximum has the code value of the experimental unit in which it is found. The count of trees is made from here by consulting the number of pixels with a fixed value. Figure 3 and 4 demonstrates an experimental unit with the maximum values included.

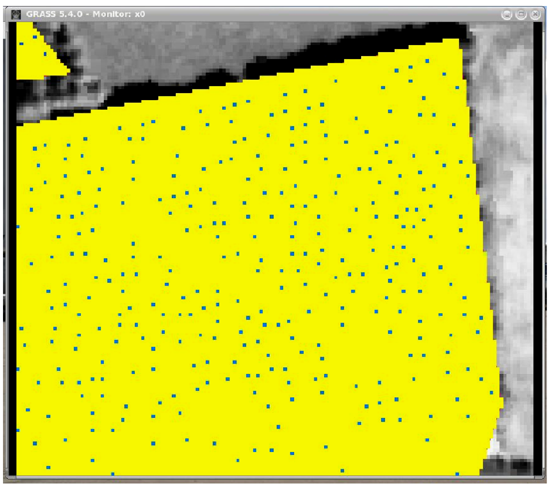

Figure 2. Detection of local maxima and

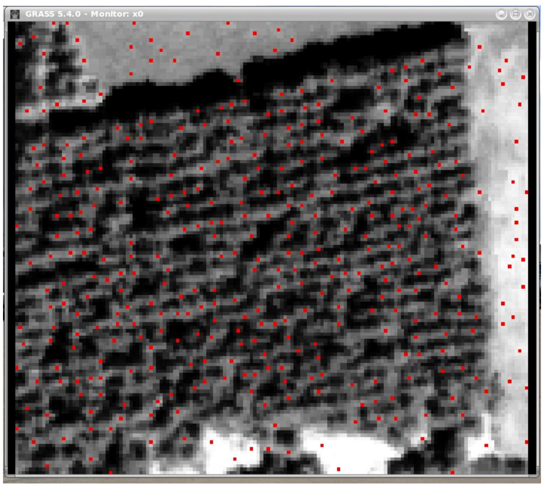

Figure 3. The assigning of local maxima to an experimental unit.

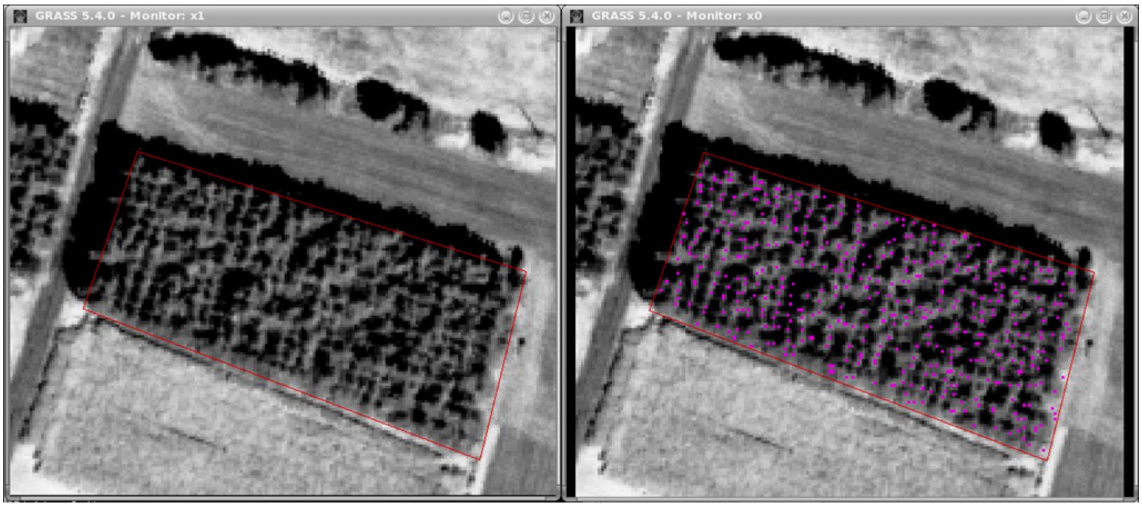

Figure 4. Represents an example of an experimental area with a corresponding mass of *Pinus radiata*.

The estimated density for each experimental unit is obtained directly by dividing the number of hectares corresponding to the area by the number of trees.

The mass density value obtained for each of the experimental units is compared with the ground surveyed value to obtain the error committed in each estimation (determined in percentage).

Table 1. Density estimated for each experimental unit (estimation 1 and estimation 2) and the committed error for each one (error 1 and error 2)

Exp. unit	Density	Species	Estimation 1	Error 1	Estimation 2	Error 2
19	1.011	*Pinus radiata*	754	-25,45	1.251	23,67
27	1.044		811	-22,40	1.216	16,40
21	1.144		718	-37,25	1.150	0,53
29	1.194		941	-21,15	1.371	14,82
30	1.260		855	-32,18	1.386	10,03
18	1.376		789	-42,66	1.284	-6,67
10	1.442		909	-36,99	1.291	-10,48
11	1.467		879	-40,07	1.242	-15,38
4b	1.547		945	-38,90	1.318	-14,81
2	895	*Eucalyptus nitens*	1.097	22,48	1.611	79,92
9	895		1.120	25,12	1.532	71,14
7	970		768	-20,77	1.086	11,97
8	995		829	-16,64	1.171	17,71
26	1.475		908	-38,48	1.474	-0,08
25	1.144	Deciduous	1.066	-6,82	1.504	31,50
5	1.376		966	-29,80	1.426	3,64
24	1.509		983	-34,86	1.438	-4,72
28	1.872		962	-48,59	1.385	-25,99
16	2.122		1.008	-52,50	1.410	-33,54
4	2.387		1.076	-54,93	1.527	-36,05

This study uses two variants of the local maxima method to identify mass densities: (1) the simplest method uses a 3x3 matrix and requires, on condition, that the central pixel has a digital number greater than those of 8 pixels and (2) a modification of the previous method aimed at adjusting upwards the values obtained. The results demonstrate that treatment 2 provides more exact global estimations than the simple method or treatment 1. (see Table 1 and 2).

Table 2. Mean error, confidence interval and standard deviation

Treatment	Mean error and confidence interval (α=0,05)	S (1)
Treatment 1	-31,21 % ; [-43,22 % , -19,20 %]	25,66 %
Treatment 2	6,67 % ; [-7,31 % , 20,64 %]	29,86 %

$$S = \sqrt{\sum_{i=1}^{n} (x_i - \bar{x})^2 / (n-1)} \qquad (1)$$

We found correlation between mass density (real) and the error committed in its estimation. In the specific case of more precise treatment (2), it was observed that significant overestimation had occurred in masses of less that 900 trees/hectare and significant underestimation in mass densities of more than 1800 trees/hectare. The first case concerns young masses with light areas which produced a high number of false positives. The second case involves masses where a high number of trees have not been identified as a result of being dominated by higher strata canopy. We have not found evidence that the specific composition of the mass has any influence on the error committed using either treatment.

Keywords: local maxima method, individual tree, forest density, Quickbird.

REFERENCES

Gougeon, F. A., Labrecque, P., Guérin, M., Leckie, D. G., Dawson, A. (2001). Détection du pin blanc dans l'Outaouais à partir d'images satellitaires à haute résolution IKONOS. *Actas do 23rd Canadian Symposium on Remote Sensing*, Ottawa.

Leckie, D. G., Burnett, C., Nelson, T., Jay, C., Walsworth, N., Gougeon, F. A., Cloney, E. 1999a. Forest parameter extraction through computer-based analysis of high resolution imagery. *Actas do 21st Canadian Symposium on Remote Sensing*, Ottawa.

Wulder, M. A., Niemann, K. O., Goodenough, D. G. 2000. Local maximum filtering for the extraction of tree locations and basal area from high spatial resolution imagery. *Remote Sensing of Environment*, 73: 103-114.

Wulder, M. A., White, J. C., Niemann, K. O., Nelson, T. 2004. Comparison of airborne and satellite high spatial resolution data for the identification of individual trees with local maxima filtering. *International Journal of Remote Sensing*, 25: 11: 2225-2232.

THE RELATIONSHIP BETWEEN DUAL POLARIZATION PALSAR DATA AND FOREST BIOMASS IN A PEAT SWAMP FOREST AFFECTED BY DRAINAGE FROM CANALS IN CENTRAL KALIMANTAN

Tomoaki TAKAHASHI[a], Yoshio AWAYA[b], Yoshiyuki KIYONO[a], Hideki SAITO[c], Suwido H. LIMIN[d], Masanobu SHIMADA[e], I Nengah Surati JAYA[f], M Buce SALEH[f], Sen NISHIMURA[a], Tamotsu SATO[a], Jumpei TORIYAMA[a]

[a] Forestry and Forest Products Research Institute, 1, Matsunosato, Tsukuba, Ibaraki, 305-8687, Japan, e-mail: tomokun@ffpri.affrc.go.jp, kiono@ffpri.affrc.go.jp, 1000n0s@gmail.com, satoo@ffpri.affrc.go.jp, jtori@ffpri.affrc.go.jp
[b] River Basin Research Center, Gifu University, 1-1 Yanagido, Gifu, 501-1193, Japan, e-mail: awaya@green.gifu-u.ac.jp
[c] Kyusyu research center, Forestry and Forest Products Research Institute, 4-11-16, Kurokami, Kumamoto, Kumamoto, 860-0862, Japan, e-mail: rslsaito@ffpri.affrc.go.jp
[d] Center for international co-operation in sustainable management of tropical peatland , Palangka Raya University, 73111, Palangka Raya, Indonesia, e-mail: cimtrop_suwido@yahoo.com
[e] Japan Aerospace Exploration Agency, 2-1-1, Sengen, Tsukuba, Ibaraki, 305-8505, Japan, e-mail: shimada.masanobu@jaxa.jp
[f] Bogor Agricultural University, 16680, Bogor, 168, Indonesia, e-mail: ins-jaya@cbn.net.id, buce_w@indo.net.id

ABSTRACT

The purpose of this study is to investigate the relationship between dual (i.e., HH and HV) polarization Phased Array type L-band Synthetic Aperture Radar (PALSAR) data and Light Detection And Ranging (LiDAR)-derived above ground biomass (AGB) in a low land peat swamp forests adjacent to Palangka Raya city in central Kalimantan in Indonesia (lat. 2.35 S, long. 114.04 E). Specifically, two types of forests exist, i.e., degraded evergreen broadleaved forests (secondary forests) and open forests (shrub land) within LiDAR-surveyed area (approximately 26 km^2) (Figure 1). The ground water level within the area has been particularly affected by the drainage from a canal constructed during the Mega Rice Project initiated between January 1996 and July 1998.

(a) (b)

Figure 1. The views of secondary forests (a) and shrub lands (b) within the LiDAR-surveyed area.

The LiDAR data were used to create a canopy height model (CHM) with a pixel size of 1 m. We estimated AGB within the LiDAR-surveyed area from the CHM using field measured eight plots' AGB data through a simple linear regression model. The PALSAR scenes used in this study were acquired on 9th July (in the middle of dry season) and 9th October (at the beginning of rainy season) 2007 and 26th May 2008 (at the end of rainy season) in dual polarization mode, with an off-nadir angle of 34.3 degrees for all scenes. The all scenes with a resolution of 12.5 m were converted from amplitude data format to sigma-naught (i.e. backscattering coefficient) (σ^0: dB). To reduce speckle effect on the images, we applied two kinds of filtering with 3 x 3 window sizes, that is, a focal mean and Lee-sigma filtering to the dual polarization images. Then we used the mesh size of 50 m in the analysis. Finally, the relationships between backscattering coefficients and LiDAR-derived AGB were investigated by nonlinear regression analysis, in which models were fitted to the data using the least-squares method. The effects of seasonal variation of PALSAR data on the relations were also investigated. The following three fitting models were used and the best fitting model was determined for each scene by using the Akaike's Information Criterion (AIC).

$$y=a_1\text{-}\exp[-(b_1 \times x+c_1)], \qquad (1)$$

$$y=a_2 \times \log(x)+b_2, \qquad (2)$$

$$y=n_3+(-17.0084 - n_3) \times \exp(-k_3 \times x), \qquad (3)$$

where a_1, b_1, c_1, a_2, b_2 ,n_3, and k_3 are the parameters estimated by the nonlinear regression analysis and -17.0084 is the mean value of the backscattering coefficients in the open forest. These three models of Eqs. (1), (2), and (3) were used in the previous studies of Balzter et al. (2003), Santos et al. (2003), and Lucas et al. (2006), respectively. X and y denote the LiDAR-derived AGB and the value of the backscattering coefficients, respectively.

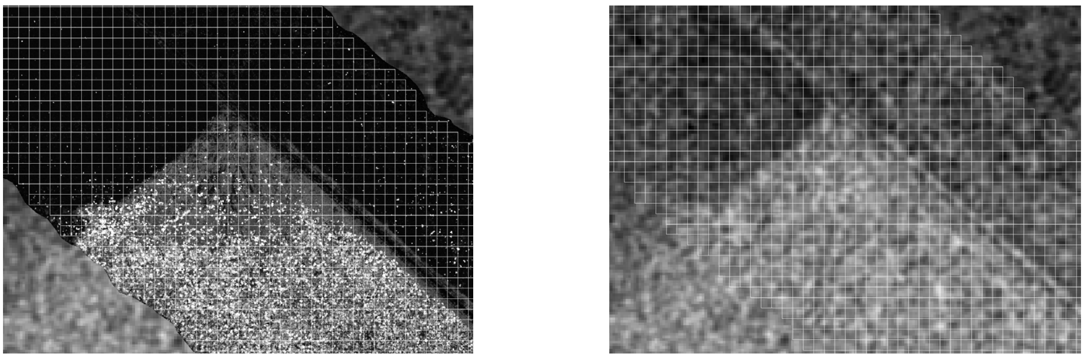

(a) (b)

Figure 2. An example of the canopy height model of LiDAR data with a resolution of 1 m (a) and PALSAR data with a resolution of 12.5m (b). White meshes denote 50 m-mesh used in the analysis. © JAXA, METI.

Figure 3 shows the example of the relationship between LiDAR-derived AGB and backscattering coefficients at 50 m-mesh size. The best fitting model was Eq.(1) for HH data, whilst Eq.(2) for HV data for all seasonal PALSAR scenes. This figure indicates that HV polarization data would be superior to HH polarization data for estimating AGB in this study area. As seen from Figures 3 and 4, HV has wider range of backscattering coefficients than that of HH. Some previous research, for example, ESA (2008) suggested that P-band gamma-naught of HV would be the most useful explanatory variable for estimating AGB. Moreover, Lucas et al. (2006) demonstrated that sigma-naught of HV derived from an airborne L-band SAR (AIRSAR) would be superior to that of HH as simple explanatory variable for estimating AGB in a secondary forest in Queensland, Australia. The residuals of the regression equations seem to have an indispensable range of approximately ±2 dB as shown in Figure 3. They are considered to be arisen from not only PALSAR data itself but also the errors of LiDAR-derived AGB, however, the range of ±2 dB was almost same as the previous research (e.g. ESA 2008; Lucas et al., 2006). Therefore, the nonlinear relationships between LiDAR-derived AGB and HV polarization data in this study seem to adversely indicate that the LiDAR-derived AGB would be appropriate values. For the future, if the reasons why and how the residuals occur could be revealed, the findings may make us improve the precision of AGB estimates from PALSAR data.

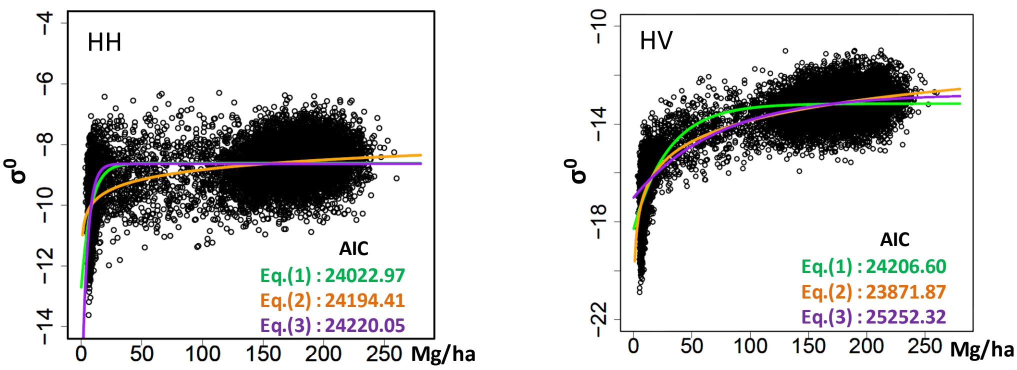

Figure 3. An example of the relationship between dual polarization data (3 x 3 focal mean filtered images acquired on 9th October 2007) and LiDAR-derived AGB. Green, orange, and purple solid lines are regression curves derived from Eqs. (1), (2), and (3) in the text, respectively.

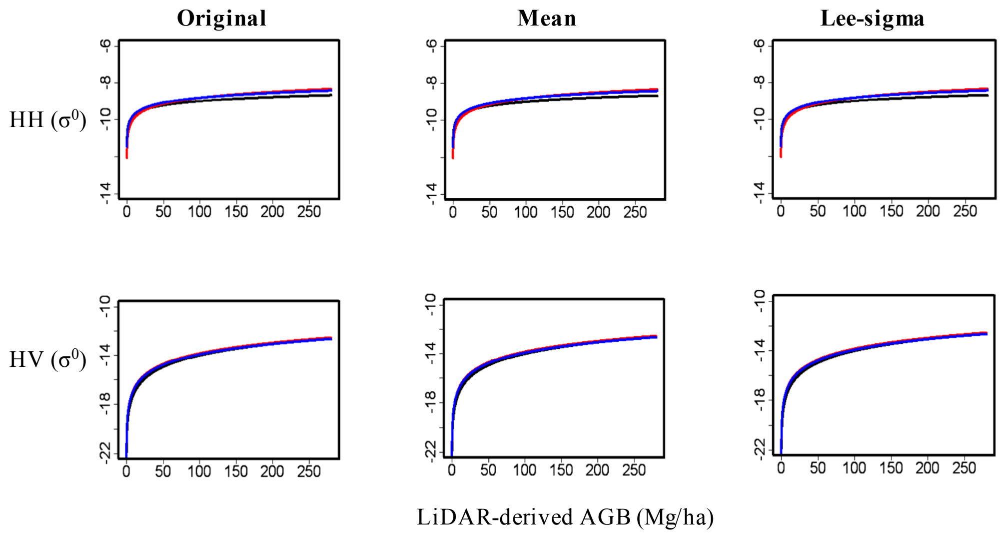

Figure 4. The relationships between LiDAR-derived AGB and dual polarization data for all images. Original means non-filtering, while Mean and Lee-sigma denote 3 x 3 focal mean and Lee-sigma filtering, respectively. Black, red, and blue solid lines are logarithmic regression curves (Eq. (2) in the text) derived from the images acquired on 9th July and 9th October 2007 and 26th May 2008, respectively.

Keywords: PALSAR, LiDAR, above ground biomass, peat swamp forest, Kalimantan.

ACKNOWLEDGMENTS

Financial support was provided by a Global Environment Research Fund (A-0802) of Ministry of the Environment, JAPAN and a Grants-in-Aid for Scientific Research (KAKENHI, No. 22780155) of Ministry of Education, Culture, Sports, Science and Technology in Japan. We thank all the CIMTROP staff for helping us to collect field data.

REFERENCES

Balzter H., Skinner L., Luckman A., Brooke R.(2003) Estimation of tree growth in a conifer plantation over 19 years from multi-satellite L-band SAR, *Remote Sensing of Environment*, 84:184-191.

ESA (2008) *Six Candidate Earth Explorer Core Missions* (Biomass), pp. 30-32.

Lucas R.M., Cronin N., Lee A., Moghaddam M., Witte C., and Tickle P. (2006) Empirical relationships between AIRSAR backscatter and LiDAR-derived forest biomass, Queensland, Australia. *Remote Sensing of Environment*, 100:407-425.

Santos J.R., Freitas C.C., Araujo L.S., Dutra L.V., Mura J.C., Gama F.F., Soler L.S., and Sant'Anna S.J.S. (2003) Airborne P-band SAR applied to the aboveground biomass studies in the Brazilian tropical rainforest, *Remote Sensing of Environment*, 87:482-493.